



# Multi-objective optimisation of engine characteristics of an RCCI diesel engine powered with Jatropa/1-pentanol blend: a Taguchi-fuzzy approach

Athmakuri Ashok<sup>1</sup> · Santhosh Kumar Gugulothu<sup>1</sup> · Ragireddy Venkat Reddy<sup>2</sup> · Srinivasa Chalapathi Kolluri<sup>2</sup>

Received: 12 January 2022 / Accepted: 22 September 2022 / Published online: 29 September 2022  
© The Author(s), under exclusive licence to Springer-Verlag GmbH Germany, part of Springer Nature 2022

## Abstract

Researchers are examining the possibilities for alternative fuel research as a fossil fuel replacement in light of global energy insecurity and other urgent challenges like global warming, severe emissions, and growing industrialization. This research uses 1-pentanol as a low reactivity fuel and Jatropa biodiesel as a high reactivity fuel to explore the reactivity-controlled compression ignition engine characteristics. A water-cooled single-cylinder engine is used in an experiment with varied loads of 25%, 50%, and 75% at a constant speed of 2000 rpm to examine the effects of operational parameters (i.e., (23 bTDC, 25 bTDC, and 27 bTDC) and (400 bar, 500 bar, and 600 bar)). The fuzzy-based Taguchi approach predicts operational parameters, including fuel injection time, fuel injection pressure, and engine load. Utilizing this ideal model, one may increase brake thermal efficiency and braking power while minimizing unburned hydrocarbon and nitrogen oxide emissions. An L20 orthogonal array is used to analyze the effects of various variables on an engine running on B20/1-pentanol fuel, including engine load, fuel injection timing, and fuel injection pressure. Multiple models are generated and verified with the use of experimental findings. Compared to other operating parameters, for reducing oxides of nitrogen, hydrocarbons, and brake-specific energy consumption maximally, engine load of 75%, FIP of 400 bar, and FIT of 23 bTDC are optimal based on the greatest MPCV value of 0.802.

**Keywords** RCCI · 1-Pentanol · Jatropa · Taguchi · Fuzzy · Engine load · FIP · And FIT

## Nomenclature

FIT	Fuel injection timing	HC	Hydrocarbon
RCCI	Reactivity-controlled compression ignition engine	CO	Carbon monoxide
FIP	Fuel injection pressure	EGR	Exhaust gas recirculation
EL	Engine load	PM	Particulate matters
BTE	Brake thermal efficiency	GHG	Greenhouse gasses
BP	Brake power	VVA	Variable value actuation
HRR	Heat release rate	LTC	Low-temperature combustion
UHC	Unburnt hydrocarbons	PCCI	Premixed charge compression ignition
BSEC	Brake-specific energy consumption	HCCI	Homogenous charge compression ignition
$P_{\max}$	Maximum pressure	EGT	Exhaust gas temperature
$\text{NO}_x$	Oxides of nitrogen	JCO	Jatropa caracus oil

Responsible Editor: Philippe Garrigues

✉ Athmakuri Ashok  
santoshgk1988@gmail.com

<sup>1</sup> Department of Mechanical Engineering, National Institute of Technology Andhra Pradesh, Tadepalligudem, India

<sup>2</sup> Department of Mechanical Engineering, ANURAG University, Hyderabad, India

## Introduction

Researchers and scientists have been researching alcohol and biodiesel as future energy sources for decades. However, the automobile industry is expected to reduce emissions to a greater extent. High density/viscosity are the disadvantages of eco-friendly, efficient, non-toxic, and sustainable vegetable oils (Dhar et al. 2012). To convert to an ester of a

low-density alkoxy group, a high-density alkoxy group of an ester was used along with alcohol and a catalyst (Schuchardt et al. 1998; Freedman et al. 1984); this process is called transesterification (Yadav et al. 2018b; Khan et al. 2017). Most countries face the technical problem of efficient and clean combustion without compromising air quality. A study published in “Nature” predicts that from 2010 to 2050, the world’s population would grow to 9 billion, i.e., a 34% increase, creating a massive need for energy (Graham-Rowe 2011).

Since 1893, biodiesel made from animal fat or vegetable oil has been used in diesel engines. Biodiesel is produced from long-chain fatty acids and is a commercial energy option for the future, contributing up to 20% of India’s renewable energy (Yadav et al. 2018a). According to researchers, biodiesel is a significant fuel source since it has diesel-identical engine combustion and more excellent lubricity. In instances, alcohol has been combined with biodiesel/diesel as an alternate energy source. Research on CI engines includes ethanol, which has been equally important in the study, among other aspects. Lee et al. (2011) investigated the influence of ethanol and hydrous ethanol in diesel engines and reported that the inclusion of ethanol reduced PM and NO<sub>x</sub> emissions significantly. An ethanol–diesel–water microemulsion’s emission and performance characteristics were studied experimentally by Qi et al. (2010).

Emissions of NO<sub>x</sub> were found to be decreased at all loading ranges, but HC and CO were found to rise. Due to low-temperature combustion, ethanol–diesel–biodiesel blends reduce smoke emissions (Zhu et al. 2013). A 4-cylinder DI (naturally aspirated) engine was used at three different air–fuel ratios and speeds by Labeckas et al. (2014). They studied emission and performance characteristics using ethanol–diesel–biodiesel at an ethanol concentration of 5–15% v/v (60 kW). As compared to the cetane number, autoignition delay is more important for the oxygenated characteristic of ethanol. At 2200 rpm, 1400 rpm, and 1800 rpm, 15% ethanol fuel emitted lower UHC and NO<sub>x</sub> than diesel. In a water-cooled direct injection single-cylinder diesel engine, the effects of higher and lower ethanol contents in an ethanol–diesel–biodiesel blend were tested by Yilmaz et al. (2014). For all blends, ethanol’s high latent heat of vaporization reduces the emission of NO<sub>x</sub>. Many researches have suggested that ethanol, when oxygenated, can decrease engine emissions and improve performance by acting as a solvent. For testing the emissions combustion and performance of a diesel engine (single-cylinder, 7 KW), up to 50%, hydrous ethanol with biodiesel–diesel can be tested. The coefficient of variation indicated mean effective pressure (COVIMEP) was found to increase by over 30% when ethanol was added at 70% load (Jamrozik et al. 2017). According to Fang et al. (2013), enhanced engine characteristics brought about by ethanol’s superior fuel qualities lead to optimum fuel–air

mixing. Brake-specific fuel consumption also increases with ethanol addition in biodiesel due to the lower heating value of biodiesel. Considering different speeds of a diesel engine (single-cylinder), i.e., 3250 rpm, 2750 rpm, 2250 rpm, and 1750 rpm, ethanol–diesel–biodiesel–cottonseed oil blends (ternary fuel) are experimentally investigated by Abulut et al. (2019). According to them, improved combustion causes lower HC and CO emissions than diesel.

Krishna et al. (2019) evaluated 17% biodiesel, 5% ethanol, and 78% diesel to obtain the best mix ratios. The study found that the optimal blend could regulate engine emissions and performance in a manner comparable to that found in diesel. Adding bioethanol to a diesel–biodiesel combination enhances the engine’s performance and minimizes pollution. This engine’s thermal and electrical efficiency could be improved by using a 3% volume of bioethanol, according to Caligiuri et al. (2019). Compared to base diesel, smoke opacity, NO<sub>x</sub>, and CO is lowered by adding 50% biodiesel to diesel. A decrease in BSFC was found when air and ethanol mixture was injected into the intake manifold in an experiment conducted by Ferreira et al. (2013). The influence of alcohol was found to be significant, i.e., it caused a reduction in inlet air temperature, due to which NO<sub>x</sub> emission decreased. However, the particulate matter and NO<sub>x</sub> emissions were reportedly increased, as Zhu et al. (2011) observed. This was caused due to delayed ignition delay because of the more extended burning phase (premixed). Shi et al. (2006) mixed biodiesel with anhydrous ethanol for studying emissions in a DI diesel engine. They found that PM emissions and THC (total hydrocarbon) decreased when speed increased.

Diesel engines need to shift to renewable from conventional fuels to address the issue of fossil fuel depletion and fulfill regulations in terms of emission. Based on the detailed literature survey, it is observed that the input variables which enhance the engine performance are different fuel injection strategies (FIP and FIT), engine load, piston bowl geometries, fuel blends, and compression ratio, respectively. It is also evident that for an RCCI engine, very few studies are conducted using the Taguchi-fuzzy-based technique to optimize the best input parameters to enhance the engine performance and decrease exhaust gasses. Therefore, the study seeks to perform tests on the RCCI engine using 1-pentanol as the low reactivity fuel and B20 (80% diesel + 20% Jatropha oil) as the high reactivity fuel. Three input factors are taken into account in the first part of the study: injection pressure (400 bar, 500 bar, and 600 bar), engine load (25%, 50%, and 75%), and injection timing (23 bTDC, 25 bTDC, and 27 bTDC). The current experimental research demonstrates precise management of input parameters is necessary to achieve the optimal engine parameters, such as emission and combustion characteristics (output parameters are essential in the study of emission and performance).

Thus, this article presents the optimal engine operating range for engine operating parameters. Multiple-variable optimization problems provide an appropriate answer for multiple objectives. So, to optimize engine emission and performance characteristics, the fuzzy-Taguchi approach is justified by the multi-objective technique. Thus, the fuzzy-logic optimization technique was used to discover the optimum operating parameters based on the maximum MPCI (multi-performance characteristics index) value.

## Research setup and methodology

The test instrument utilized in the experiment is shown in Fig. 1. On an RCCI engine, the experiment was conducted with various loads (25 to 75%) at a constant speed of 2000 rpm. The investigation is carried out to learn how fuel injection variables affect the engine's performance and combustion characteristics. An eddy current dynamometer is used to maintain a constant speed and varying load. Additionally, the setup was a CRDI system for FIP and FIT maintenance. Table 1 lists the engine's technical parameters. Only a necessary quantity of gasoline is pressurized tanks to the

placement of an intake valve. The pressure is controlled, and a high-frequency signal turns on the spill valves. Due to the lack of a 16-bit controller and needed spill flow, pressure is controlled by a high-pressure valve (supplementary). A pressure sensor is mounted to the rail to monitor and adjust the pressure, and a pressure transducer (quick reacting) is also put between the rail and the injector to permit high-pressure data. The test platform is set up with four Bosch-supplied common rail injector ports that can handle 100 MPa pressure and 18 cm<sup>3</sup> volume. On one side of the tube, a pressure sensor is installed that collects data for closed-loop injection pressure management as well as for timing and flow calculations. It uses a Delphi 3-hole injector (solenoid) that can inject 0.5 to 100 mg of fuel each injection (20–100 MPa range). However, a second fuel injection system (secondary FIS) is required when combustion is carried out in RCCI mode. A fuel accumulator, a fuel injector control circuit, an electric fuel pump, a fuel injector, and a fuel tank make up this supplementary fuel injection equipment (Table 2). The fuel injection system operates at a 3 bar injection pressure. The outcomes of a gas analyzer's analysis of the NO<sub>x</sub> and unburned HC emission characteristics are shown in Table 2. Unburned HC was measured as a volume percentage, while

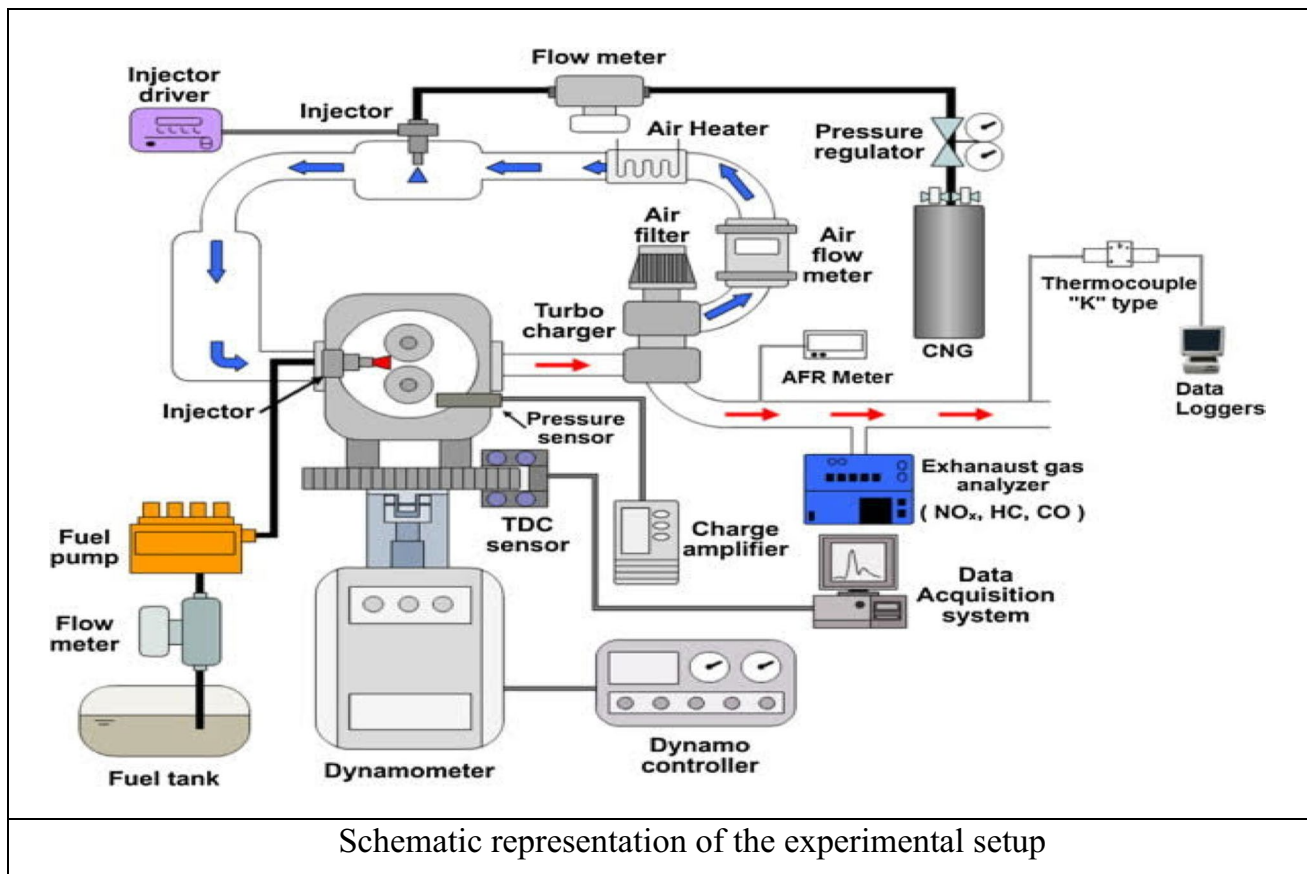


Fig. 1 Schematic representation of the experimental setup

**Table 1** Specification details of the engine [23–24]

Make	Kirloskar
Product	Common Rail DI engine (computerized)
Number of cylinders	One
Stroke (mm) and bore (mm)	110 and 87.5
Cubic capacity (cc)	661
Speed (rpm)	1500
Power (kW)	3.5
Dynamo meter	Eddy current, water-cooled with loading unit
Fuel injector	Solenoid driven
Calorimeter	Pipe in pipe type
Electronic control unit (nira)	i7r
Piezo sensor	Make PCB; combustion range: 350 bar
Temperature sensor	RTD
Crank angle sensor	Data acquisition
Load sensor	Strain gauge
Fuel flow transmitter	DP transmitter
Air flow transmitter	Pressure transmitter
Temperature transmitter	Two wires: I/P RTD PT100, O/P 4–20 amps
Rotameter	Engine jacket 40–400 LPH, calorimeter 25–250 LPH

**Table 2** Properties of fuel used

Properties	Fuels		
	D100	1-pentanol	Jatropha oil
Chemical composition	HC (C <sub>10</sub> to C <sub>21</sub> )	C <sub>5</sub> H <sub>12</sub> O	
Density (kg/m <sup>3</sup> )	820	814.8	880
Kinematic viscosity (cSt)	2.416	2.89	40.4
Cetane number	53	18.15	52.1
Calorific value (MJ/kg)	43.168	34.65	38.91
Water content (ppm)	12	14	13
Oxygen content (%)	0.04	0	8.97
Flash point (°C)	60	54	168

NO<sub>x</sub> was recorded in ppm (fixed into the engine exhaust). Testo-350 gas analyzers were fixed to the engine's exhaust during the trial phase to measure the amount and calculate the NO<sub>x</sub> and unburned hydrocarbons. A display and stopwatch were also used to calculate the fuel intake. As shown

in Table 3, there may be up to five gas analyzers employed. Using only regular diesel fuel, the engine is run for 30 min to stabilize and keep it warm (Stone 1992; Panda et al. 2018; Yasar et al. 2015).

## Experimental methodology

To create a baseline reading, the tests are first carried out by altering the engine load by increasing it from 25 to 100% with a 25% increment while using pure diesel. Then, experiments are carried out in dual fuel mode on RCCI engines with diesel mixed with Jatropha oil as the high reactivity fuel and 1-pentanol being delivered via the intake manifold as the low reactivity fuel at each load increment at the standard FIT of 25°bTDC and FIP of 400 bar. Additionally, studies are carried out with various fuel injection pressures (400–600 bar) at the standard injection time (25°bTDC) at part load and full load to improve fuel injection parameters.

**Table 3** Uncertainty analysis of instruments used in experiments

Equipment	Make	Range	Accuracy	Uncertainty (%)
Gas analyzer	AVL	CO: 0–10%	±0.01	±0.5
		HC: 0–20,000 ppm	±1 ppm	±0.7
		NO <sub>x</sub> : 0–5000 ppm	±1 ppm	±0.3
Crank angle sensor	Kubler	0–360°	±1° CA	±0.2
Load cell	Sensortronics	0–50 kg	±0.1 kg	±0.1
Load indicator	ABUS Technologies	0–100 kg	±0.2%	±0.2
RPM indicator with speed sensor	Selection process control	4–9999 rpm	±0.05%	±2.0
Pressure transducer	PCB Piezotronics	5000 psi	±0.1 psi	±0.2

Similarly, the CRDI configuration is used to investigate various fuel injection timings ( $23^\circ\text{bTDC}$ ,  $25^\circ\text{bTDC}$ , and  $27^\circ\text{bTDC}$ ) at a constant FIP of 400 bar. Once the engine stabilizes, an emission analyzer is added to the exhaust to capture data on emissions. To guarantee a constant flow rate, the calorimeter and engine water flow rates are continuously monitored. To increase the precision of the measurements, ten readings are recorded for each piece of data. To prevent any cyclical variations, the data is gathered over an average of 80 cycles.

## Results and discussion

These paper tests are conducted on modified CRDI engines operating in RCCI mode using B20 (80% diesel + 20% Jatropha oil) as the primary fuel and 1-pentanol as the secondary fuel. B20 is a highly reactive fuel. Fuel injection time and pressure variations are tested while maintaining a steady speed under both partial and full loads. The premixed lower-reactive charge mixture is injected into the air intake stream before being introduced into the combustion chamber. After the compression stroke, highly reactive fuel was introduced immediately into the combustion chamber. The injected higher-reactive fuel was then ignited by the lower-reactive fuel–air combination that had been premixed. The RCCI engine's combustion, performance, and emission analysis is obtained.

## Engine combustion analysis

A high-speed data acquisition system is employed to gather the pressure data related to the position of the crank angle. Analysis of cylinder pressure data is the best way to investigate combustion properties in a combustion chamber. Net Heat Release Rate is the thermal energy rate released during fuel combustion in the engine (Ramachander et al. 2021a; Sahin and Durgun 2009; Seelam et al. 2022; Sivaramakrishnan and Ravikumar 2012). During the combustion cycle, when combustion analysis is conducted, HRR is an important parameter to consider. It can identify ignition delay, knocking and flameout period, etc. The variation in crank angle position with respect to cylinder pressure and HRR at different engine loads (25–75%) is depicted in Fig. 2 at an FIP of 400 bar, 500 bar, and 600 bar. Maximum HRR is noted when maximum combustion occurs inside the combustion chamber due to a rise in injection pressure at all loads. However, the peak HRR stays away from the Top Dead Center (TDC) when the load increases. The peak HRR increased by 13.7%, 15.2%, and 12.8%, and the in-cylinder pressure was seen to increase by 7.6%, 8.2%, and 8.6% when the injection pressures (IP) increased slowly from 400 to 600 bar. This is due to an increase in the in-cylinder pressure with an increase in injected fuel pressure, resulting in the acceleration of fuel droplets vaporization leading to air–fuel mixture homogeneity. An

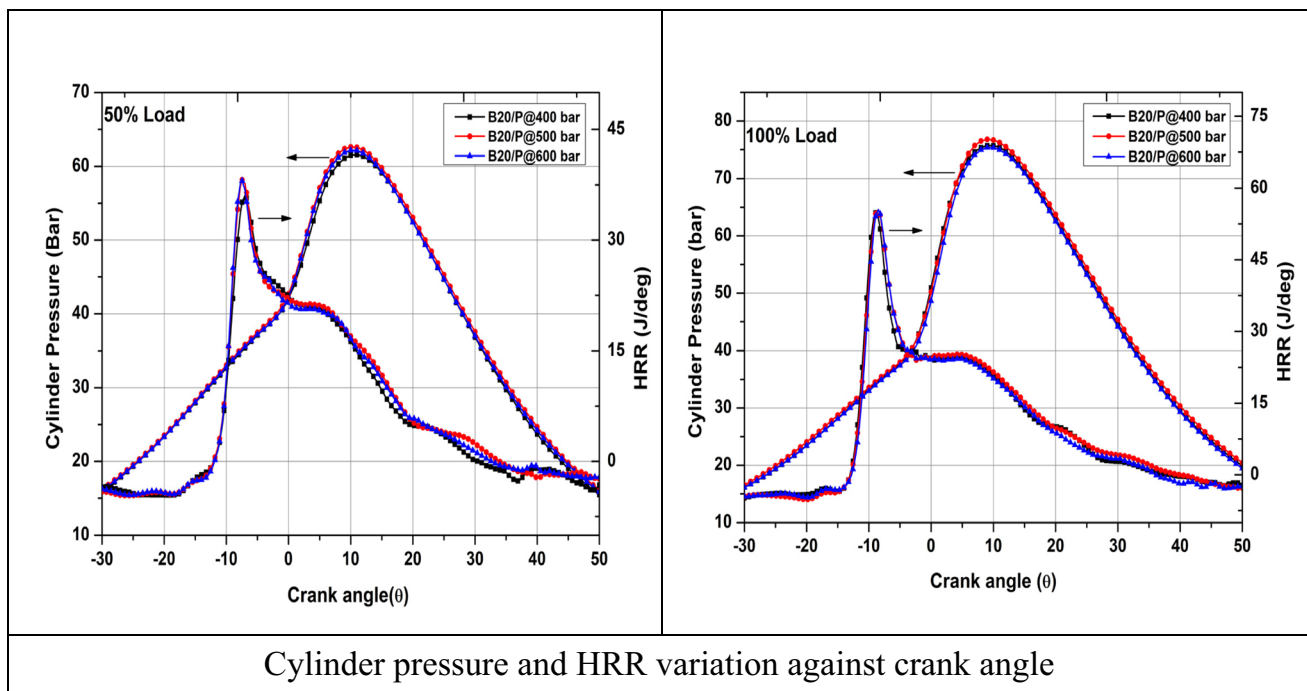


Fig. 2 Cylinder pressure and HRR variation against crank angle

increase in IP facilitates complete combustion, resulting in a higher heat release. It further encourages better contact with fuel droplets owing to an increase in the surface area of droplets.

For different timings of fuel injection (23 bTDC, 25 bTDC, and 27 bTDC) and standard injection pressure of 500 bar, crank angle variation with respect to cylinder pressure and HRR is shown in Fig. 3. Because of the longer ignition delay and higher cylinder pressure caused by the higher injection pressure (500 bar), the maximum heat release rate is achieved at 27°bTDC. A higher burning proportion is observed because of the shorter ID, allowing more fuel to be burned in the combustion chamber at a lower peak IP at SOI 23°bTDC. A prolonged ignition delay at FIP of 500 bar, coupled with maximum cylinder pressure and adequate premixed combustion, results in a maximum rate of heat release. The considerably shorter ignition delay period at SOI 27°bTDC, on the other hand, results in complete combustion in the combustion chamber at lesser in-cylinder pressure. In comparison to the other two injection timings and the lower maximum pressure, the peak pressure moves away from TDC toward the combustion stroke when the FIT is retarded (Rahman et al. 2015; Ramachander et al. 2021b; Ramachander and Gugulothu 2022a, b). With SOI 23°bTDC, the peak of HRR curves visibly shifts away from TDC. The figure demonstrates that due to the high net calorific value and outstanding fuel atomization characteristics, all loads have the highest HRR.

## Engine performance characteristics

### Brake thermal efficiency

The variation in BTE at different engine loads (25–75%) is depicted in Fig. 4a at an FIP of 400 bar, 500 bar, and 600 bar. It is observed that with an increase in the engine load, BTE also increased for all the injection pressures. Compared to other FIPs, the maximum BTE is observed in the case of 600 bar FIP at all engine loads. BTE at all the loads is observed due to the inclusion of 1-pentanol in the blend. This is due to the presence of adequate oxygen molecules leading to complete combustion (Nutakki and Gugulothu 2022; Panda et al. 2017; Paul et al. 2013, 2016; Qi et al. 2011). However, as still, the BTE of the blend is lesser, it can be overcome by increasing the FIP. Simultaneously, when the evaporation rate is enhanced and physical delays are decreased, the BTE and combustion efficiency are improved. Compared with the other FIPs, better BTE is observed in the case of 600 bar FIP at all engine loads.

The variation in BTE at different engine loads (25–75%) is depicted in Fig. 4b at an FIT of 23°bTDC, 25°bTDC, and 27°bTDC. At advanced injection timing, better BTE is observed at all the engine loads compared to standard and retarded injection timings. This is due to better atomization leading to complete combustion. Due to advancements in the FIT, the process of atomization is improved which helps to improve the premixed stage of combustion. The addition of 1-pentanol, too, enhances the combustion process.

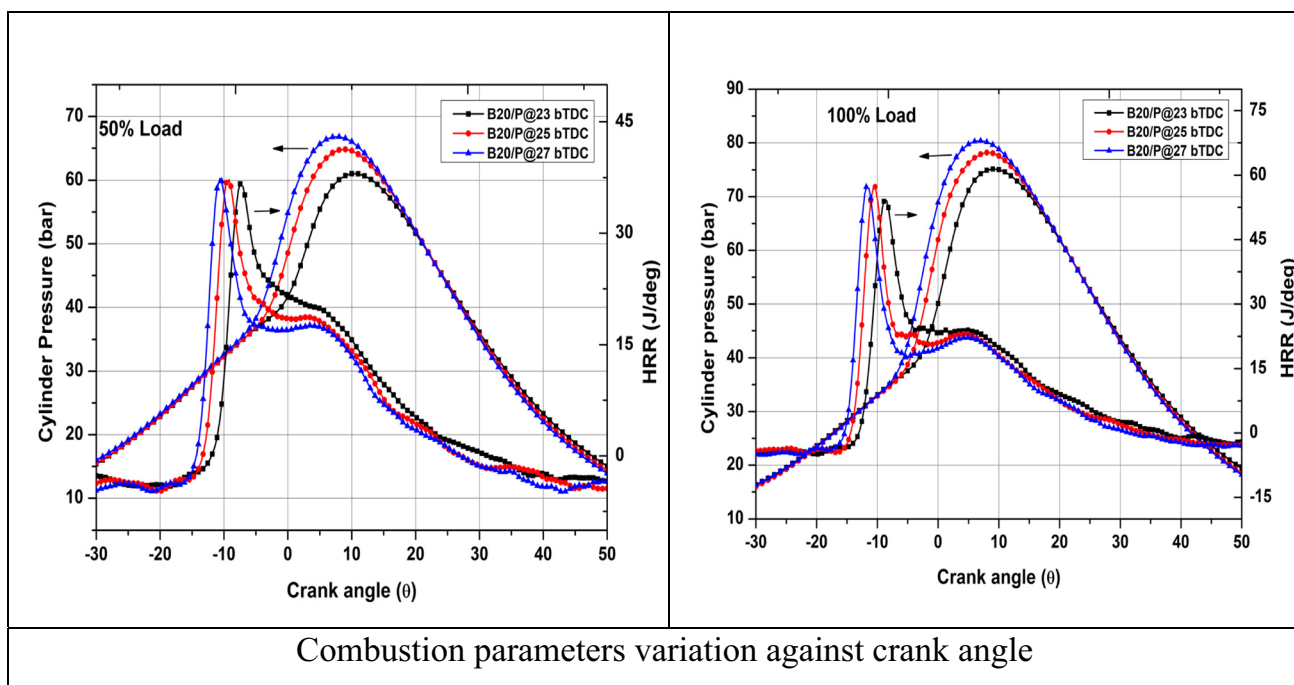
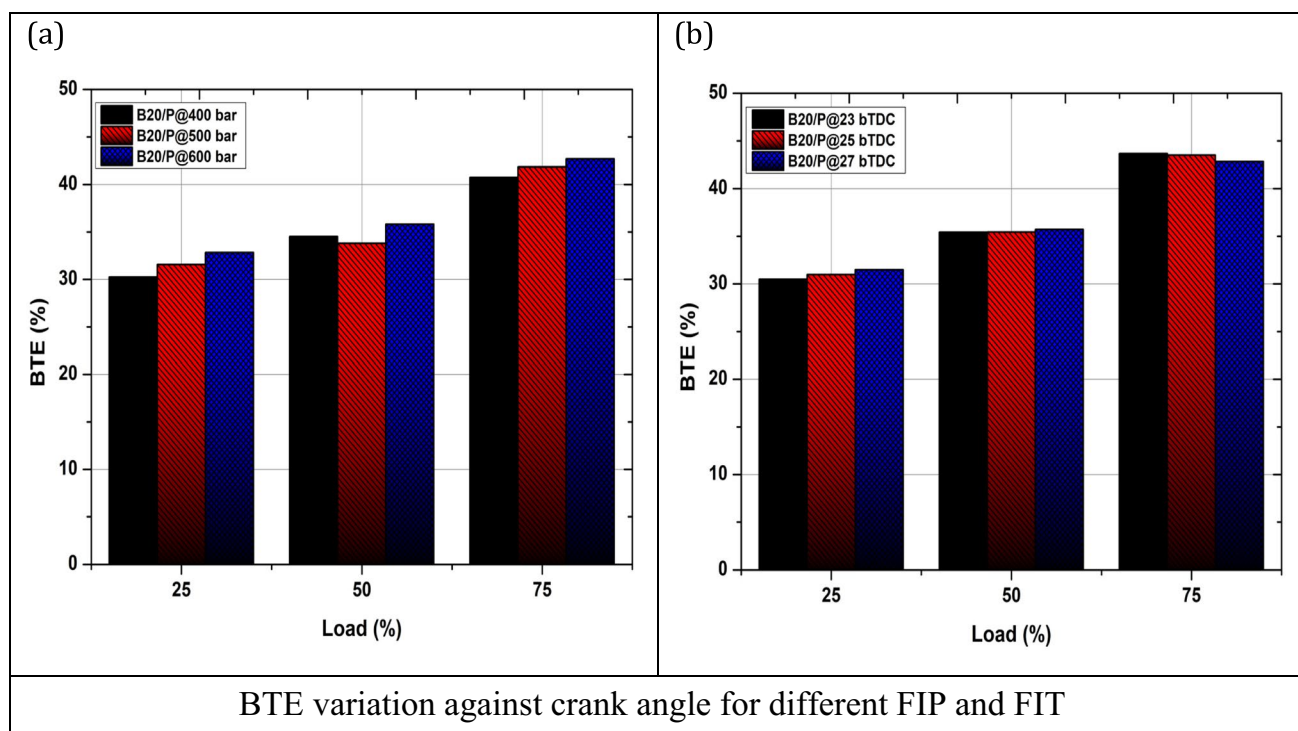


Fig. 3 Combustion parameters variation against crank angle



**Fig. 4** BTE variation against crank angle for different FIP and FIT

BTE attained 44.42% of the threshold value at the FIT of 27°bTDC and 500 bar injection pressure. The 2 to 3.8% improvement in the BTE was brought on by the change in injection time from 23 to 27°bTDC. However, at lower injection time, cylinder pressure impacts the fuel spray distribution since the greater droplet size brought on by atomization tends to evaporate slowly.

### Engine emission analysis

Figure 5a, b depicts the variation of HC and NO<sub>x</sub> emissions against engine load at different FIP of 400 bar, 500 bar, and 600 bar. When the combustion quality is top-notch, fewer unburned hydrocarbons are formed, and vice versa. The unburnt HC decreased by 16.3%, 13.2%, and 8.3%, respectively. Complete combustion occurs when FIP increases and accurate fuel–air blending happens, which eventually decreases the emission of exhaust gases. Nitric oxide is an important compound as it is the primary reason behind smog, acid rains, and other environmental issues. The generation of NO<sub>x</sub> is mainly determined by the oxygen quantity in the pilot fuel, the injection of fuel, the residence time under maximum temperature, the heating value, and the cetane number. It was found that NO<sub>x</sub> emissions increased with FIP enhancement at varying engine loads. A rise of 32.4% in NO<sub>x</sub> emissions is observed at an engine load of 75% and injection pressure of 600 bar. As a result of the

increased rate of heat release during premixed combustion, which predominates in the NO<sub>x</sub> chemical reaction, the FIP of 600 bar results in higher maximum NO<sub>x</sub> emissions than the FIP of 400 bar. The major factors affecting the generation of NO<sub>x</sub> are available time for chemical reaction, oxidation, and exhaust gas temperature (Kumar Bose and Banerjee 2012; Labeckas et al. 2014; Nagi and Khaleel Ahmed 2016). After studying the NO<sub>x</sub> emission response of the engine, it was clear that compared to all other factors, the effect of the engine load is predominant, followed by FIP. It was observed that when engine load increases (for every injection pressure), there is a corresponding increase in NO<sub>x</sub> emission. Figure 6a, b depicts the HC and NO<sub>x</sub> emission formation variation against engine load with different fuel injection timings. At SOI 27°bTDC, NO<sub>x</sub> emissions were observed to be increased due to a prolonged ignition delay and extended time for chemical reaction, as compared to the other two SOI values. HC emissions also follow a similar pattern due to accurate blending of the fuel–air mix at higher loads and high temperatures inside the cylinder. All of these lead to an increase in the emissions of unburnt hydrocarbons and better combustion.

### Trade-off study (engine characteristics)

Giving up one quality, quantity, or attribute in exchange for another is referred to as a trade-off. The trade-off

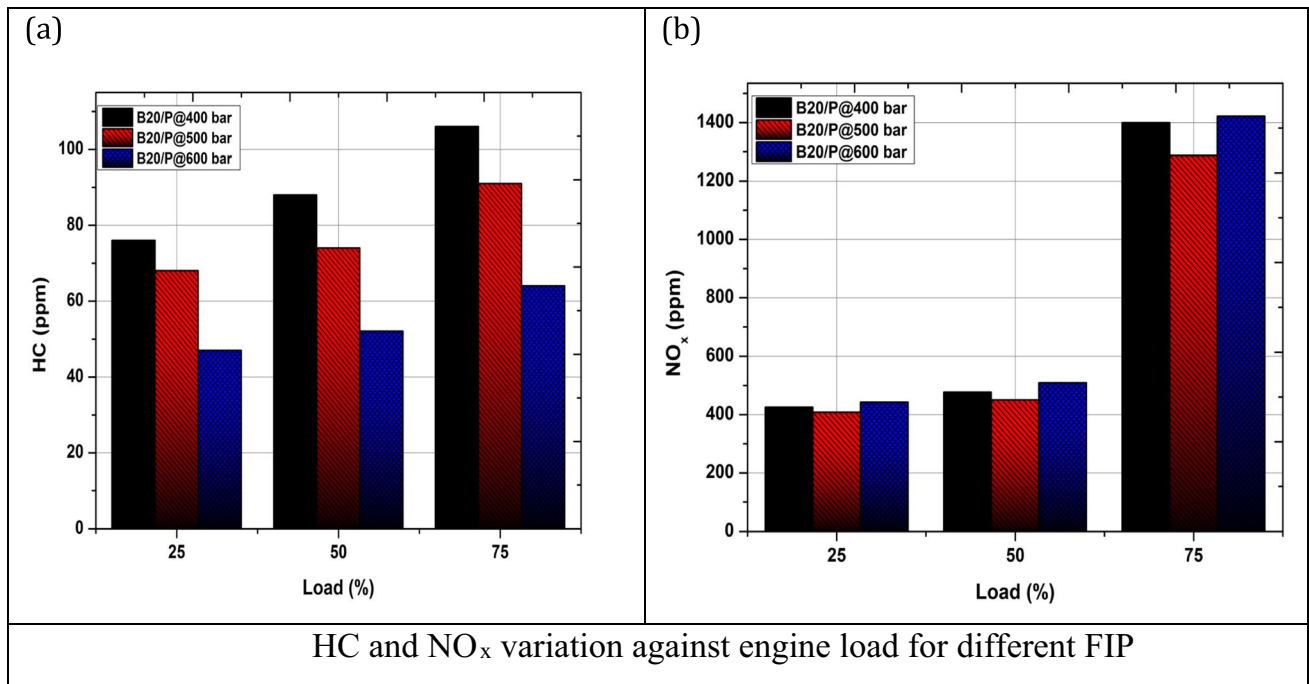


Fig. 5 HC and NO<sub>x</sub> variation against engine load for different FIP

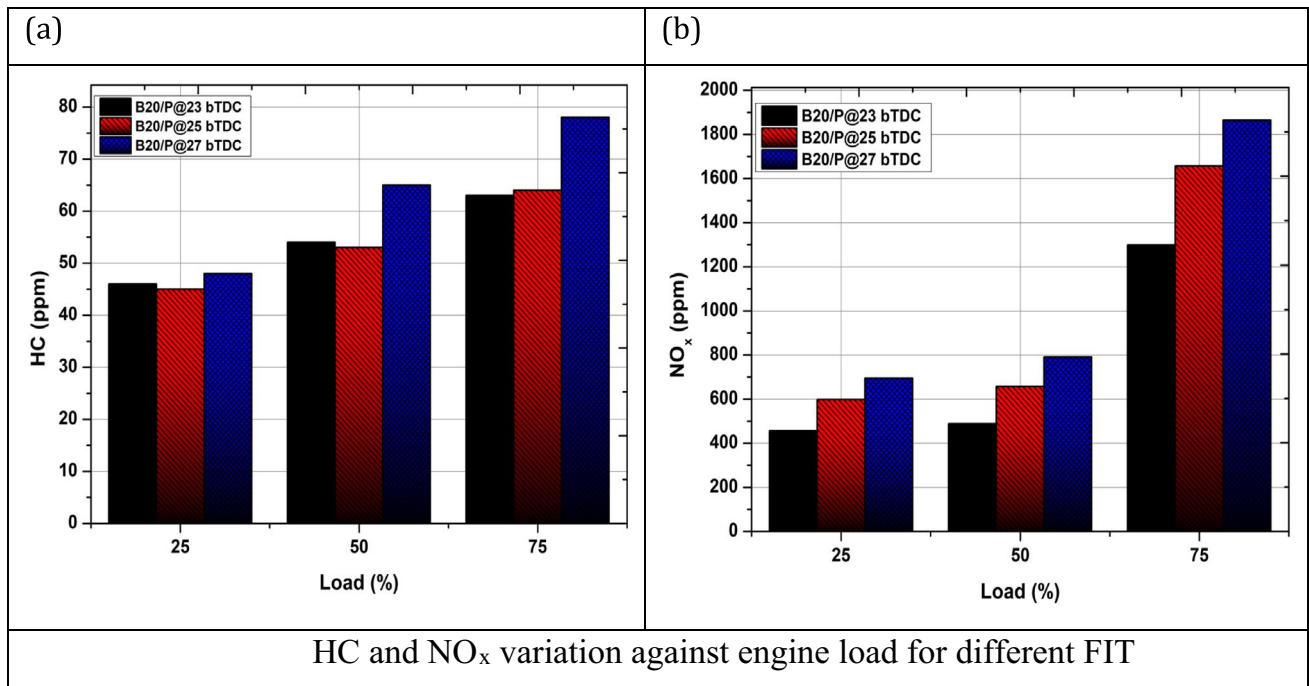
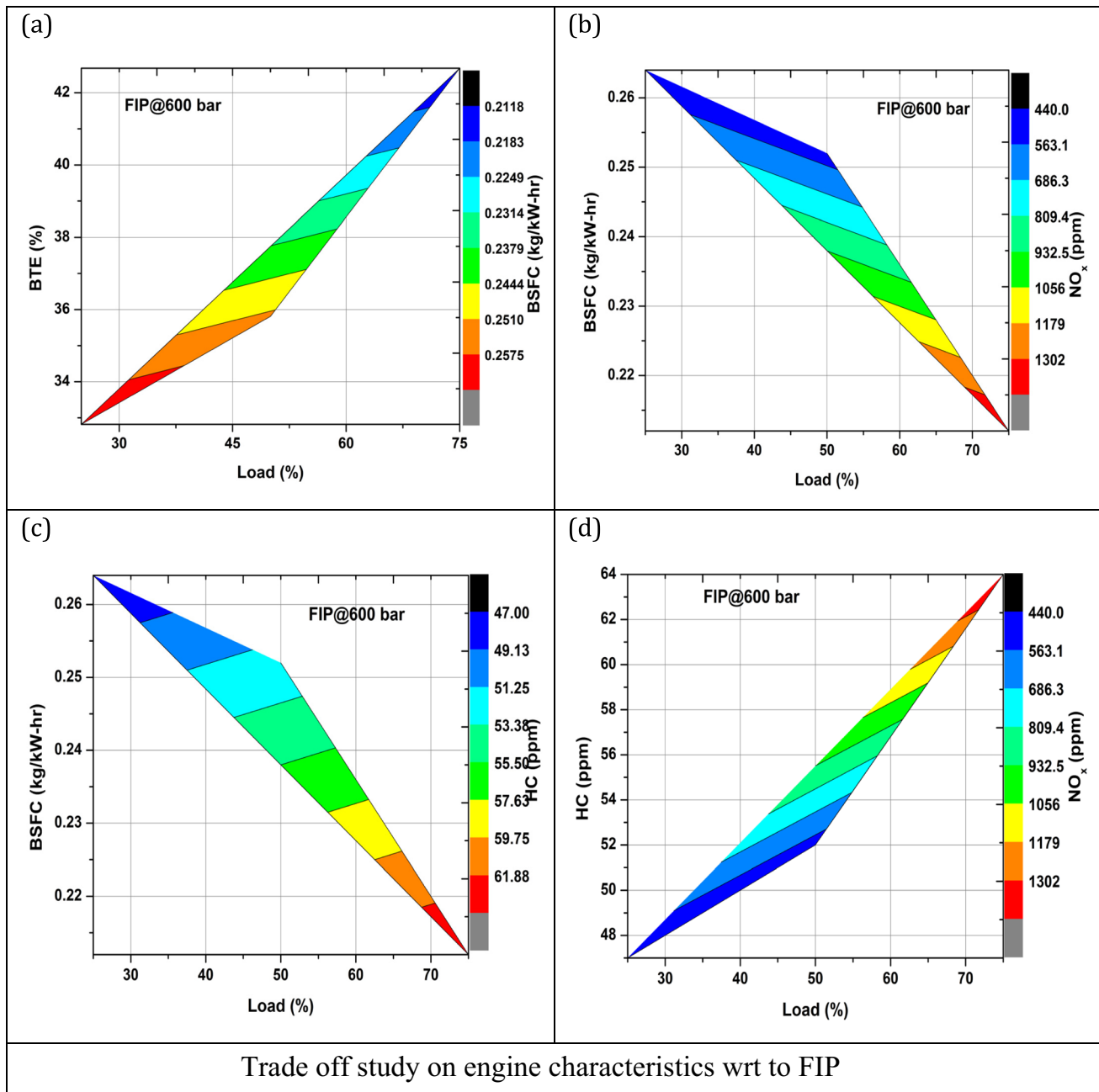


Fig. 6 HC and NO<sub>x</sub> variation against engine load for different FIT

is made even more unusual by endeavoring to lessen one footprint while increasing another. Diesel engine designers have created several complex technological

improvements in response to the present problems with forced trade-offs. Figure 7 displays a comparison of emission and performance data. The BSFC and BTE trade-offs





**Fig. 7** Trade-off study on engine characteristics wrt to FIP

change depending on engine load, as shown in Fig. 7a. Due to the persistence of combustion, it is seen that when engine load increases, the maximum BTE shifts to the right corner (Dewangan et al. 2018; Dhar et al. 2012; Ganapathy et al. 2009; Kishore and Gugulothu 2021). When utilizing oxygenated alcohol and biodiesel, 1-pentanol-diesel-Jatropha oil blends perform better under higher and medium loads. As the load rises, the improved fuel–air combination causes full combustion, raising the

temperature and pressure within the cylinder. The highest emission of UHC and  $\text{NO}_x$  occurs in the D and E zones, with  $\text{NO}_x$  vs. BSEC and UHC vs. BSEC being the trade-offs for loads (Fig. 7). When load grows to high from low shown at the right bottom of the plot. Zone F shows a very low emission of UHC at low to medium load. As shown in zones H and G,  $\text{NO}_x$  and UHC are seen to be minimal and maximal at higher as well as lower loads [ $\text{NO}_x$  versus UHC trade-off at various loads (Fig. 7d)].

### Multi-objective optimization of operating parameters by adopting Taguchi-fuzzy-based approach

For finding optimum performance parameters in a diesel engine, Taguchi's DOE is one of the best theoretical techniques (Wu and Wu 2013). One of the important characteristics of the method is its ability to change the value of data repetition by varying it (Ganapathy et al. 2009). Taguchi's method is able to evaluate the SNR (signal-to-noise ratio) using statistical design analysis and an orthogonal array. SNR was chosen as the performance parameter in this investigation. Using an orthogonal array, this method aims on varying the individual parameters at the same time to observe their effect on performance. As per Taguchi, three numerical possibilities are defined for the factor effects: higher-the-better, nominal-the-better, and lower-the-better. According to Karnwal et al. 2011, Eqs. (1) and (2) indicate the important parameters of higher-the-better and lower-the-better. As given in Eq. (2), SNR

is calculated to reduce NO<sub>x</sub>, UHC, and BSFC by using the lower-the-better expression in this paper.

$$S/N = -10\log\left(\frac{1}{N_i} \sum_{u=1}^{N_i} \frac{1}{y_u^2}\right) \tag{1}$$

where  $N_i$  is the number of trials for experiment,  $u$  is the trial number, and  $i$  is the experiment number.

$$\text{Smaller - the - better} = S/N = -10\log\left(\frac{1}{n} \sum_{i=0}^n y_i^2\right) \tag{2}$$

“ $n$ ” = measurements, “ $y$ ” =  $i$ th value.

### SNR (S/N ratio) analysis

Within a small experimental matrix, the desired response variables effect is dependent on the large number of design factors which is studied by using Taguchi's method which used an orthogonal array. The orthogonal array usage provides the shortest possible matrix where a combination of different variations of parameters is represented for finding out its direct effect on output. They also reduce the number of experiments to be conducted (Aydin and Ilkilic 2010; Banerjee et al. 2015; Deb et al. 2014). Due to the self-balancing nature of orthogonal arrays, the conclusions drawn from experiments (scaled) whose validity are based on the range of control variables under observation. The selection of design factors (load, FIP, and FIT) was done

**Table 4** Control factors and their level of experiments

Parameters	Units	Level 1	Level 2	Level 3
Load	Nm	25	50	75
Inj. timing (bTDC)	°CA	23	25	27
FIP	bar	400	500	600

**Table 5** Taguchi's orthogonal array (L<sub>20</sub>) with MPCII value

Sl. No	Load	FIT	FIP	BP	BTE	NO <sub>x</sub>	UHC	MPCII
				(Normalized)				
1	50	25	500	0.489	0.72	0.213	0.318	0.43
2	50	27	500	0.502	0.77	0.296	0.045	0.40
3	50	25	500	0.498	0.73	0.243	0.273	0.44
4	75	27	400	0.987	0.96	0.936	0.000	0.72
5	50	25	400	0.489	0.71	0.154	0.318	0.42
6	75	23	600	0.997	0.93	0.899	0.273	0.78
7	50	25	500	0.486	0.72	0.255	0.273	0.43
8	75	27	600	1.000	1.00	1.000	0.045	0.76
9	50	25	500	0.483	0.75	0.247	0.273	0.44
10	25	23	600	0.009	0.01	0.022	0.955	0.25
11	50	25	600	0.514	0.76	0.232	0.227	0.43
12	75	25	500	0.943	0.93	0.948	0.182	0.75
13	25	23	400	0.000	0.00	0.000	1.000	0.25
14	<b>75</b>	<b>23</b>	<b>400</b>	<b>0.956</b>	<b>0.90</b>	<b>0.876</b>	<b>0.455</b>	<b>0.80</b>
15	25	27	400	0.006	0.00	0.034	0.364	0.10
16	25	27	600	0.009	0.02	0.079	0.273	0.09
17	50	23	500	0.489	0.71	0.176	0.545	0.48
18	50	25	500	0.492	0.72	0.255	0.227	0.42
19	25	25	500	0.003	0.00	0.026	0.636	0.17
20	50	25	500	0.502	0.72	0.251	0.318	0.45

Bold values are the best combination to maximize efficiency, and reduce emissions

to find out their effect on desired response variables of BP, BTE, HC, and  $\text{NO}_x$  which has been studied extensively in this paper. Each factor was assigned three levels. As illustrated in Table 4, the operating parameters and their level of experiments are mentioned. And as per Table 4, a 20-row Taguchi L20 orthogonal array was constructed which corresponds to the number of trials illustrated in Table 5. Using smaller-the-better, the Taguchi approach selects  $\text{NO}_x$ , UHC, as operational factors for obtaining SNRs. Table 4 shows the SNRs of emission and performance characteristics normalized between 0 and 1, estimated using L20 orthogonal arrays for calculation of overall quality characteristics. The SNR equation used for normalization is given below (Panda et al. 2017; Ashok et al. 2022b, c, d; Athmakuri et al. 2022):

$$x_{\text{normalized}} = \frac{(x_i - x_{\min})}{(x_{\max} - x_{\min})} \quad (3)$$

### Fuzzy-based approach

The fuzzy-based optimization approach is a popular active optimization technique developed by adopting the core

fundamentals of the fuzzy algorithm (Zadeh 1961). Previously in engineering research and industries, optimization based on fuzzy logic was widely used. In their study, Bose et al. (2013) used triangle membership functions and conducted fuzzy division on output and input variables to find MPCCI values (Fig. 8). Basically, the fuzzy analysis is classified into defuzzification, fuzzy interface engine, fuzzy rule base, etc. Small (S), medium (M), and large (L) are the subsets of  $\text{NO}_x$ , UHC, and BTE (input variables). This fuzzy system generates a fuzzy linguistic subset as MPCCI, which ranges from 0 to 1. MPCCI is then converted to a fuzzy linguistic subset using the triangular membership function (Panda et al. 2018). It has been determined that the output variable has been divided into seven distinct subsets, each of which represents a different level of severity (Sakthivel and Ilangkumaran 2017). Very very high (VVH), very very low (VVL), very high (VH), very low (VL), high (H), low (L), and medium (M) are the seven subsets. Table 6 lists the 81 fuzzy rules that were chosen for all output and input levels. To discover the optimal factor combination, the SNR curves for BP, BTE, HC, and  $\text{NO}_x$  are represented graphically (Fig. 9). Fuzzy-based optimization shows the highest MPCCI value of 0.80 with the factor combination of 75% load, 23 FIP,

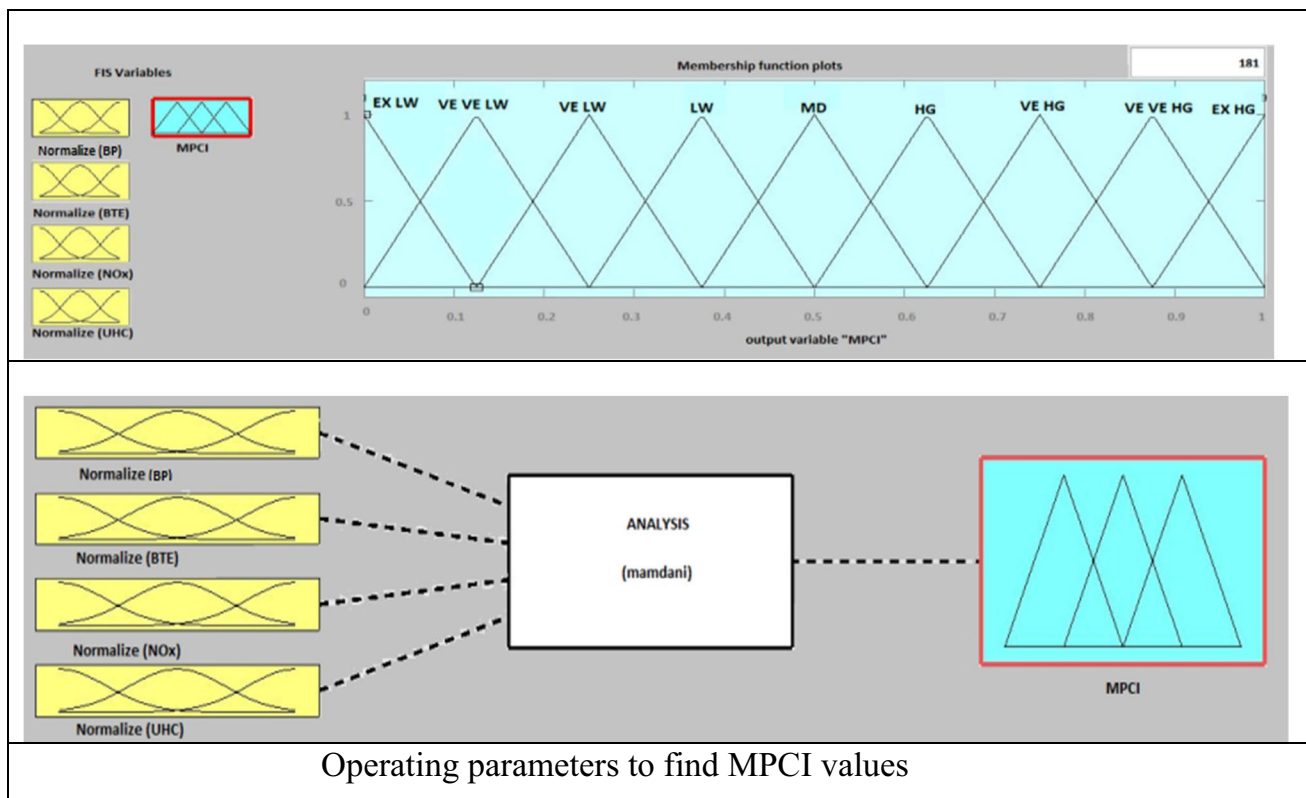


Fig. 8 Operating parameters to find MPCCI values

**Table 6** Fuzzy rule for response variables

SI. NO	BP	BTHE	UHC	NO <sub>x</sub>	MPCI
1	LW	LW	LW	LW	EX LW
2	LW	LW	LW	MD	VE VE LW
3	LW	LW	MD	LW	VE VE LW
4	LW	LW	LW	HG	VE LW
5	LW	LW	HG	LW	VE LW
6	LW	LW	MD	MD	VE LW
7	LW	LW	MD	HG	LW
8	LW	LW	HG	MD	LW
9	LW	LW	HG	HG	MD
10	LW	MD	LW	LW	VE VE LW
11	LW	MD	MD	LW	VE LW
12	LW	MD	LW	MD	VE LW
13	LW	MD	MD	MD	LW
14	LW	MD	HG	LW	LW
15	LW	MD	LW	HG	LW
16	LW	MD	HG	MD	MD
17	LW	MD	MD	HG	MD
18	LW	MD	HG	HG	HG
19	LW	HG	LW	LW	VE LW
20	LW	HG	LW	MD	LW
21	LW	HG	MD	LW	LW
22	LW	HG	HG	LW	MD
23	LW	HG	LW	HG	MD
24	LW	HG	MD	MD	MD
25	LW	HG	MD	HG	HG
26	LW	HG	HG	MD	HG
27	LW	HG	HG	HG	VE HG
28	MD	LW	LW	LW	VE VE LW
29	MD	LW	LW	MD	VE LW
30	MD	LW	MD	LW	VE LW
31	MD	LW	LW	HG	LW
32	MD	LW	HG	LW	LW
33	MD	LW	MD	MD	LW
34	MD	LW	MD	HG	MD
35	MD	LW	HG	MD	MD
36	MD	LW	HG	HG	HG
37	MD	MD	LW	LW	VL
38	MD	MD	LW	MD	LW
39	MD	MD	MD	LW	LW
40	MD	MD	LW	HG	MD
41	MD	MD	HG	LW	MD
42	MD	MD	MD	MD	MD
43	MD	MD	MD	HG	HG
44	MD	MD	HG	MD	HG
45	MD	MD	HG	HG	HG
46	MD	HG	LW	LW	LW
47	MD	HG	LW	MD	MD
48	MD	HG	MD	LW	MD
49	MD	HG	LW	HG	HG
50	MD	HG	HG	LW	HG

**Table 6** (continued)

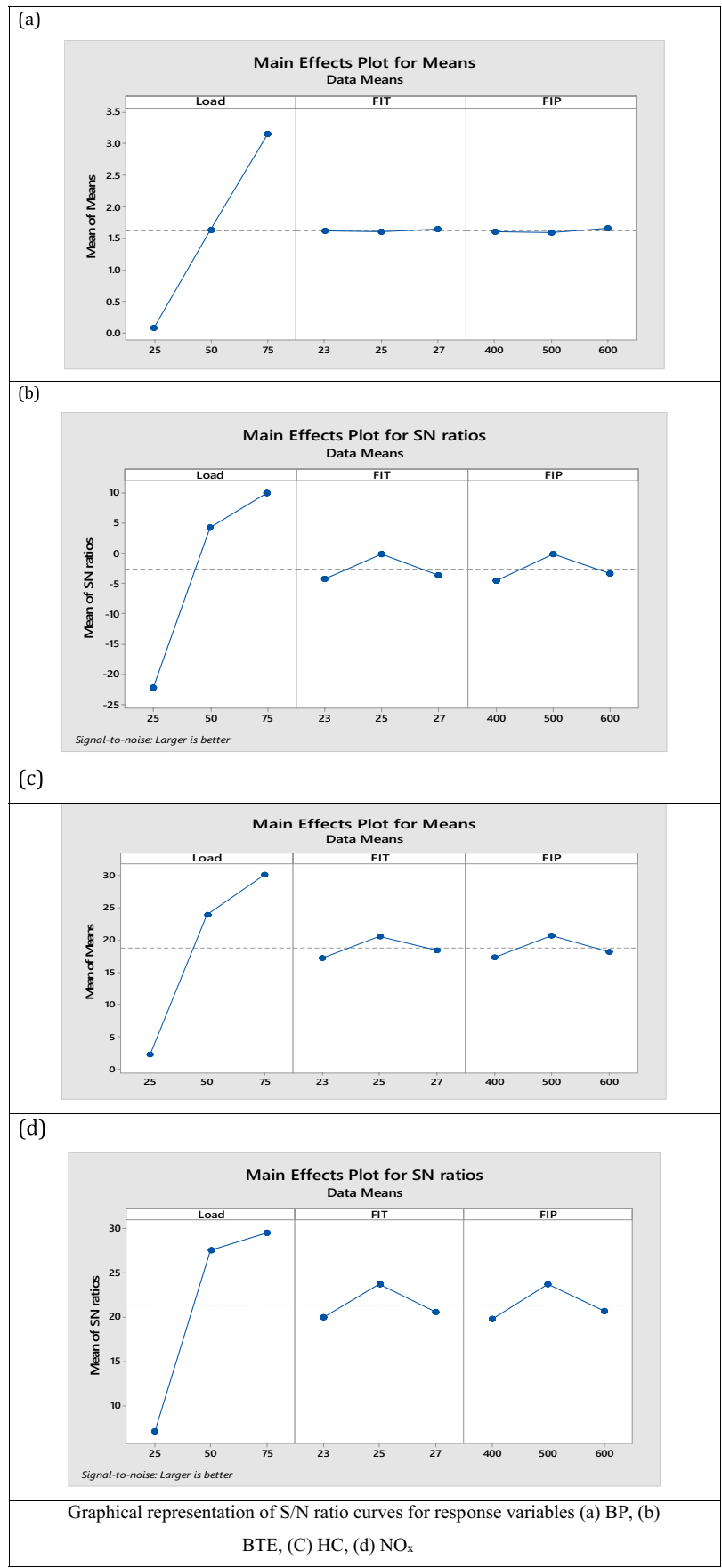
SI. NO	BP	BTHE	UHC	NO <sub>x</sub>	MPCI
51	MD	HG	MD	MD	HG
52	MD	HG	MD	HG	VE HG
53	MD	HG	HG	MD	VE HG
54	MD	HG	HG	HG	VE VE HG
55	HG	LW	LW	LW	VE LW
56	HG	LW	LW	MD	LW
57	HG	LW	MD	LW	LW
58	HG	LW	LW	HG	MD
59	HG	LW	HG	LW	MD
60	HG	LW	MD	MD	MD
61	HG	LW	MD	HG	HG
62	HG	LW	HG	MD	HG
63	HG	LW	HG	HG	VH
64	HG	MD	LW	LW	LW
65	HG	MD	LW	MD	MD
66	HG	MD	MD	LW	MD
67	HG	MD	LW	HG	HG
68	HG	MD	HG	LW	HG
69	HG	MD	MD	MD	HG
70	HG	MD	MD	HG	VE HG
71	HG	MD	HG	MD	VE HG
72	HG	MD	HG	HG	VE VE HG
73	HG	HG	LW	LW	MD
74	HG	HG	LW	MD	HG
75	HG	HG	MD	LW	HG
76	HG	HG	LW	HG	VE HG
77	HG	HG	HG	LW	VE HG
78	HG	HG	MD	MD	VE HG
79	HG	HG	MD	HG	VE VE HG
80	HG	HG	HG	MD	VE VE HG
81	HG	HG	HG	HG	EX HG

and 400 FIT, which signifies the better performance with controlled emissions compared to other blends (Abu-Hamdeh and Alnefaie 2015; Agbulut et al. 2019; Ashok et al. 2022a).

### Conclusions

To assess the emissions and performance characteristics of the RCCI engine powered with 1-pentanol as the low reactivity fuel and B20 (80% diesel + 20% Jatropha oil) as the high reactivity fuel with different operating parameters are considered. Taguchi-fuzzy-based optimization techniques using numerical methods were used for determining the optimal input components for obtaining lower emissions and higher engine performance. The impact on output responses

**Fig. 9** Graphical representation of S/N ratio curves for response variables: (a) BP, (b) BTE, (C) HC, and (d) NO<sub>x</sub>



of input variables has been investigated using experimental data. Output responses such as NO<sub>x</sub> emissions, HC, NHRR, BTE, and BP were predicted by fuzzy-based models. The study's primary findings are as follows.

- Using experimental operational factors including FIP, FIT, and engine load, the fuzzy-made linear prediction model accurately forecasted and covered changes in emission characteristics and engine combustion.
- It was found that the optimal load, injection pressure, and injection timing for the engine were 75%, 400 bar, and 23°bTDC, respectively. The normalized NO<sub>x</sub>, hydrocarbon, BTE, and BP values were 0.876, 0.455, 0.90, and 0.956, respectively, in the above setup.
- NO<sub>x</sub> emission does not alter at high, low, or medium loads. However, UHC emissions increase. This is due to incomplete combustion caused by 1-pentanol's low cetane number.
- To explain the effect of operating parameters (engine load, FIP, and FIT) on NO<sub>x</sub>, HC, BTE, and BP in the Taguchi method, SNR curves are employed.
- The greatest MPC<sub>I</sub> was 0.802 using the triangular membership function for fuzzy optimization.

The study concluded that a 75% engine load, 400 bar injection pressure, and 23°bTDC fuel injection timing powered with B20/1-pentanol has the best emission and performance characteristics compared to other operating parameters in a multi-objective optimization technique (fuzzy-based). Thus, the fuzzy-Taguchi approach works well in these scenarios.

**Author contribution** Santhosh Kumar Gugulothu: conceptualization, procedure, writing – review and editing, supervision; Athmakuri Ashok: experimental analysis, procedure, and writing; Ragireddy Venkat Reddy: supervision; Srinivasa Chalapathi Kolluri: analysis exploration and documentation.

**Data availability** The data acquired or analyzed during this investigation are incorporated in this article.

## Declarations

**Ethics approval** The simulation analysis has not harmed any human or animal. National and international guidelines are followed for the protection of social welfare.

**Consent to participate** Not applicable.

**Consent for publication** We affirm that the article has been studied and accepted by all listed authors. In addition, we affirm that all the authors mentioned in the article have been approved by all of us.

**Competing interests** The authors declare no competing interests.

## References

- Abu-Hamdeh NH, Alnefaie KA (2015) A comparative study of almond and palm oils as two bio-diesel fuels for diesel engine in terms of emissions and performance. *Fuel* 150:318–324. <https://doi.org/10.1016/j.fuel.2015.02.040>
- Ağbulut Ü, Sarıdemir S, Albayrak S (2019) Experimental investigation of combustion, performance and emission characteristics of a diesel engine fuelled with diesel – biodiesel – alcohol blends. *J Braz Soc Mech Sci Eng* 41:1–12. <https://doi.org/10.1007/s40430-019-1891-8>
- Ashok A, Gugulothu SK, Reddy RV, Burra B (2022a) Influence of 1-pentanol as the renewable fuel blended with Jatropha oil on the reactivity-controlled compression ignition engine characteristics and trade-off study with variable fuel injection pressure. *Sustain Energy Technol Assess* 52:102215
- Ashok A, Gugulothu SK, Reddy RV, Burra B (2022b) Influence of fuel injection timing and trade-off study on the RCCI engine characteristics of Jatropha oil-diesel blend under 1-pentanol dual-fuel strategies. *Environ Sci Pollut Res* 1–10. <https://doi.org/10.1007/s11356-022-22039-3>
- Ashok A, Gugulothu SK, Reddy RV, Burra B, Panda JK (2022c) A systematic study of the influence of 1-pentanol as the renewable fuel blended with diesel on the reactivity controlled compression ignition engine characteristics and trade-off study with variable fuel injection pressure. *Fuel* 322:124166
- Ashok A, Gugulothu SK, Reddy RV, Gurel AE, Deepanraj B (2022d) Prediction-optimization of the influence of 1-pentanol/Jatropha oil blends on RCCI engine characteristics using multi-objective response surface methodology. *Renew Energy Focus* 42:8–23
- Athmakuri A, Gugulothu SK, Reddy RV (2022) Box-Behnken response surface methodology based multi-objective optimisation on reactivity controlled compression ignition engine characteristics powered with ternary fuel. *J Energy Resour Technol* 1–24
- Aydin H, İlkiliç C (2010) Effect of ethanol blending with biodiesel on engine performance and exhaust emissions in a CI engine. *Appl Therm Eng* 30(10):1199–1204. <https://doi.org/10.1016/j.applthermaleng.2010.01.037>
- Banerjee R, Roy S, Bose PK (2015) Hydrogen-EGR synergy as a promising pathway to meet the PM-NO<sub>x</sub>-BSFC trade-off contingencies of the diesel engine: a comprehensive review. *Int J Hydrogen Energy* 40:12824–12847
- Bose PK, Deb M, Banerjee R, Majumder A (2013) Multi objective optimization of performance parameters of a single cylinder diesel engine running with hydrogen using a Taguchi-fuzzy based approach. *Energy* 63:375–386. <https://doi.org/10.1016/j.energy.2013.10.045>
- Caligiuri C, Renzi M, Bietresato M, Baratieri M (2019) Experimental investigation on the effects of bioethanol addition in diesel-biodiesel blends on emissions and performances of a micro-cogeneration system. *Energy Convers Manage* 185:55–65. <https://doi.org/10.1016/j.enconman.2019.01.097>
- Deb M, Majumder A, Banerjee R, Sastry GRK, Bose PK (2014) A Taguchi-fuzzy based multi-objective optimization study on the soot-NO<sub>x</sub>-BTHE characteristics of an existing CI engine under dual fuel operation with hydrogen. *Int J Hydrogen Energy* 39(35):20276–20293. <https://doi.org/10.1016/j.ijhydene.2014.09.171>
- Dewangan A, Yadav AK, Mallick A (2018) Current scenario of bio-diesel development in India: prospects and challenges. *Energy Sources, Part A: Recovery, Util Environ Eff* 40(20):2494–2501. <https://doi.org/10.1080/15567036.2018.1502849>
- Dhar A, Kevin R, Agarwal AK (2012) Production of biodiesel from high-FFA neem oil and its performance, emission and combustion



- Shi X, Pang X, Mu Y, He H, Shuai S, Wang J, Chen H, Li R (2006) Emission reduction potential of using ethanol–biodiesel–diesel fuel blend on a heavy-duty diesel engine. *Atmos Environ* 40(14):2567–2574. <https://doi.org/10.1016/j.atmosenv.2005.12.026>
- Sivaramakrishnan K, Ravikumar P (2012) Performance optimization of Karanja biodiesel engine using Taguchi approach and multiple regressions. *ARP J Eng Appl Sci* 506–516
- Stone R (1992) Introduction to internal combustion engines. Macmillan Press, Hampshire
- Tutak AW, Pyrc M, Sobiepanski M (2017) Effect of diesel-biodiesel-ethanol blend on combustion, performance, and emissions characteristics on a direct injection diesel engine. *Thermal Science* 21(1 Part B):591–604. <https://doi.org/10.2298/TSCI160913275J>
- Wu H-W, Wu Z-Y (2013) Using Taguchi method on combustion performance of a diesel engine with diesel/ biodiesel blend and port-inducting H<sub>2</sub>. *Appl Energy* 104:362–370. <https://doi.org/10.1016/j.apenergy.2012.10.055>
- Yadav VS, Tripathi S, Singh AR (2018a) Bi-objective optimization for sustainable supply chain network design in omnichannel. *Journal of Manufacturing Technology Management* 30(6):972–986
- Yadav AK, Vinay V, Singh B (2018b) Optimization of biodiesel production from *Annona squamosa* seed oil using response surface methodology and its characterization. *Energy Sources, Part A: Recovery, Util Environ Eff* 40(9):1051–1059. <https://doi.org/10.1080/15567036.2018.1468516>
- Yasar A, Bilgili M, Yildizhan S (2015) The influence of diesel-biodiesel-alcohol blends on the performance and emissions in a diesel engine. *Int J Sci Technol Res* 1:52–61
- Yilmaz N, Vigil FM, Donaldson AB, Darabseh T (2014) Investigation of CI engine emissions in biodiesel– ethanol–diesel blends as a function of ethanol concentration. *Fuel* 115:790–793. <https://doi.org/10.1016/j.fuel.2013.08.012>
- Zadeh LA (1961) Time-varying networks, I. *Proceedings of the IRE* 49(10):1488–1503
- Zhu L, Cheung CS, Zhang WG, Huang Z (2011) Combustion, performance and emission characteristics of a DI diesel engine fueled with ethanol–biodiesel blends. *Fuel* 90(5):1743–1750. <https://doi.org/10.1016/j.fuel.2011.01.024>
- Zhu H, Bohac SV, Nakashima K, Hagen LM, Huang Z, Assanis DN (2013) Effect of biodiesel and ethanol on load limits of high-efficiency premixed low-temperature combustion in a diesel engine. *Fuel* 106:773–778. <https://doi.org/10.1016/j.fuel.2012.10.073>

**Publisher's note** Springer Nature remains neutral with regard to jurisdictional claims in published maps and institutional affiliations.

Springer Nature or its licensor holds exclusive rights to this article under a publishing agreement with the author(s) or other rightsholder(s); author self-archiving of the accepted manuscript version of this article is solely governed by the terms of such publishing agreement and applicable law.